NANO LETTERS

2008
Vol. 8, No. 4
1076-1080

Examination of Nanoparticles via Single Large Cluster Impacts

S. Rajagopalachary, S. V. Verkhoturov, and E. A. Schweikert*

Department of Chemistry, Texas A&M University, College Station, Texas 77842-3012

Received November 24, 2007; Revised Manuscript Received February 11, 2008

ABSTRACT

This study deals with the determination of the relative abundance of the oxide layer in the near-surface volume of aluminum nanoparticles of 50–100 nm in diameter. They are bombarded with a sequence of single projectiles of Au_{400}^{4+} accelerated to 136 keV. The ionized ejecta from each impact are recorded individually which allows identification of ions emitted from a surface volume of ~10 nm in diameter and 5–10 nm in depth. The mode of analyzing ejecta individually from each single cluster impact is a means to apply mass spectrometry in nanovolumes.

The characterization of the near-surface of nanoparticles poses the challenge of detecting molecular species within nanometric dimensions. We address here this issue with a variant of secondary ion mass spectrometry, SIMS, which differs from customary SIMS in the type of projectile and mode of operation. In the study described below, nanoparticles were bombarded with a sequence of single massive projectiles, specifically hypervelocity Au_{400}^{4+}. It is well-documented that surfaces bombarded with high-energy clusters show enhanced emission of molecular ions.[1,2] A further distinction in our experiment is that the ionized ejecta or secondary ions, SIs, from each impact were mass-analyzed and recorded individually. Under these conditions, one observes the SIs emitted from the volume perturbed by one projectile impact, i.e., an area of ~10 nm in diameter and a depth of 5–10 nm.[3,4] Such coemitted SIs can thus reveal information about molecules colocated in a nanovolume.[5,6]

The goal of this study was to determine the relative abundance of oxide layer in the near-surface volume of aluminum nanoparticles nominally coated with a self-assembled monolayer, SAM, of palmitic acid. More explicitly, the particles (high combustion rate propellant) are prepared with a controlled oxide layer and then coated with the SAM to prevent further oxidation (Figure 1). In practice, the coverage with the SAM may not be complete, thus prompting degradation of the particles when exposed to air. We show below that the sorting of SIs from a sequence of single Au_{400}^{4+} impacts on nanoparticles allows an assessment of the relative SAM coverage and comparison of the overall oxide layer with those in areas covered by the SAM (Figure 2). It must be noted that the data presented are from samples of nanoparticles deposited on a metal substrate, resulting in a layer that is a few micrometers thick. The projectiles probe the sample stochastically in a nonimaging mode.

* Corresponding author. E-mail: Schweikert@mail.chem.tamu.edu.

10.1021/nl0730716 CCC: $40.75
Published on Web 03/01/2008

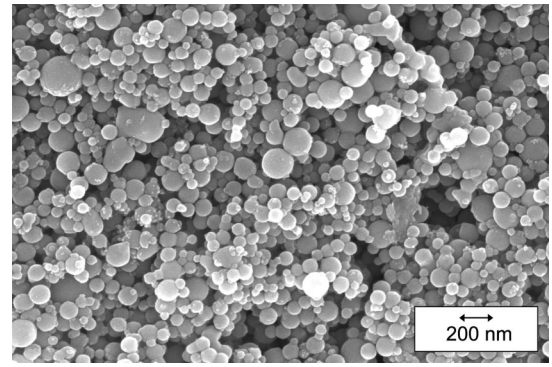

Figure 1. Micrograph of analyte obtained by SEM. The Al nanoparticles (average size ~50 nm) are nominally coated with a self-assembled monolayer of palmitic acid (layer thickness ~2–3 nm). The micrograph obtained for the oxidized particles is identical and has the same deposition morphology.

Three different batches of Al nanoparticles (Argonide Corp.) were investigated: nanoparticles coated by a SAM of palmitic acid with an average diameter of 50 nm (specimen A); 100 nm nanoparticles coated by a SAM of palmitic acid (specimen B); and oxidized nanoparticles (not coated) with an average diameter of 50 nm (specimen C). The nanoparticles were shipped and stored in an argon atmosphere. They were dissolved in acetone at 25 mg/mL and sonicated. A 25 μL aliquot of the solution was deposited on a metal substrate. The thickness of the nanoparticle layer (a few micrometers) on the substrate was larger than the depth of secondary ion emission (~10 nm). Figure 1 shows the scanning electron microscope (SEM) image of the coated Al nanoparticles (average size 50 nm). It should be noted that SEM is unable to distinguish between the coated and the uncoated particles. The nanoparticles were briefly exposed to air (~10 min) during deposition on the substrate and insertion into the mass spectrometer.

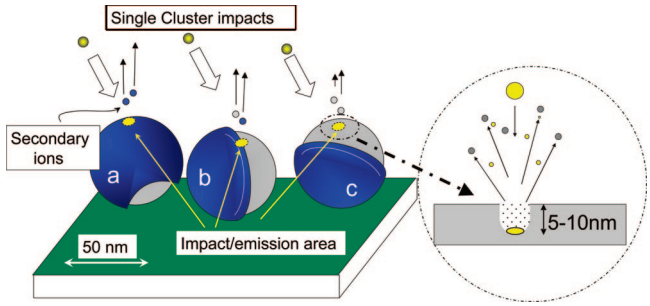

Figure 2. Schematic illustration of the analysis of nanoparticle surface areas. The aluminum nanoparticles (size ~50 nm) were slightly oxidized before they were coated by a self-assembled monolayer (SAM) of palmitic acid. SAM-coated areas are indicated in blue color. The uncoated areas (gray) are aluminum oxide layers. Single impacts of large gold cluster ions (136 keV Au_{400}^{+}) stimulate the emission of the secondary atomic, molecular, and cluster ions. The emission area is a nanodomain of ~10 nm in depth. The type of emitted ions depends on the area of a single impact.

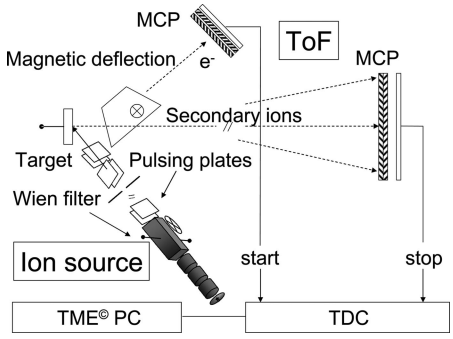

Figure 3. Schematic of the Cluster SIMS instrument with the Au LMIS. The 136 keV Au_{400}^{+} projectiles generated by the ion source strike the target (nanoparticles deposited on the metal substrate) at a repetition rate of ~1000 impacts/s. The secondary electrons are emitted from single cluster impacts, deflected by the weak magnetic field, and detected by the dual microchannel plate (MCP) detector. The pulse from this detector serves as the start signal for the time-of-flight measurement of secondary ions. The secondary ions are detected by another set of dual MCP detector. The pulse from this detector constitutes the stop signal. The start and stop signals are fed into a time-to-digital converter (TDC), its output is stored in a PC as individual mass spectra by the TME software.[9]

The experiments were run on a Cluster SIMS instrument comprising of a liquid metal ion source, a Wien filter for primary ion mass selection, a beam pulser for single projectile bombardment, and a linear time-of-flight mass spectrometer (Figure 3).[7] The liquid metal ion source, LMIS, procured from the Institute of Nuclear Physics Orsay (France), produces gold clusters in a wide range of masses.[8] The reference cited gives details on the production and identification of heavy gold clusters. The protocol followed for producing the large cluster ions has been described earlier.[7] For the mass selection of the primary cluster ions, we used a combination of the Wien filter with subsequent selection by time-of-flight. The time-of-flight selection of the primary cluster ions was performed with two pulse generators, specifically, a high-voltage pulser and a gate generator.[7] The mass/time selected cluster projectiles used in this study are Au_{400}^{4+} accelerated to 136 keV. The secondary ions were detected with a dual microchannel plate, MCP, assembly. All impact/emission/detection events (typically ~2×10^6 events) are collected and stored as a "total matrix of events", TME, described elsewhere.[9]

The performance of SIMS with single large cluster impacts is demonstrated below on different samples of the specimens A, B, and C. Two types of mass spectra of negatively charged SIs were obtained: the normal one and the spectrum of SIs coemitted with the deprotonated molecular ion of palmitic acid ($m/e = 255$) (Figure 4 and Figure 6, respectively). The normal mass spectra are presented in Figure 4. These mass spectra in the lower mass range have common peaks which correspond to the aluminum oxide layer.[10] The prominent peaks are at $m/e = 43$, attributed to AlO^-, and at $m/e = 59$, attributed to AlO_2^-. In the higher mass range, the mass spectrum shows repeating units of cluster ions. Some of them are oxide-specific ions while others are hydroxide specific ions with different base units. These clusters match with ones found in literature.[10] The clusters can be classified into three different groups, namely, $[(Al_2O_3)_nAlO_2]^-$, $[(Al_2O_3)_nOH]^-$, and $[AlO_2(AlO)_n(OH)_n]^-$. The aluminum oxide clusters are present, despite the coverage of these particles by a monolayer of palmitic acid, because the palmitic acid layer is only 2–3 nm in thickness. The depth of secondary ion emission however for the Au_{400}^{4+} projectile is ~10 nm in organic layers.[3] The most abundant cluster (in terms of both intensity and number) is $[(Al_2O_3)_nAlO_2]^-$. In our experiments, the least abundant cluster group is $[AlO_2\ (AlO)_n\ (OH)_n]^-$, where n does not exceed 4. Returning to the mass spectrum of the nanoparticles from the specimen A (Figure 4a), a peak that can be attributed to the deprotonated molecule from the palmitic acid (m/e 255) is visible, in between the two clusters of $[AlO_2(AlO)_3(OH)_3]^-$ ($Al_4O_8H_3$ in Figure 4 inset) and $[(Al_2O_3)_2(AlO)(OH)_2]^-$ ($Al_5O_9H_2$ in Figure 4 inset). The assignment of this peak to palmitic acid is verified by the cluster SIMS analysis of palmitic acid (Sigma Aldrich) which shows the deprotonated molecule at $m/e = 255$. The mass spectrum of the coated nanoparticles A is similar to the spectrum of the coated particles B in terms of the presence of clusters, but the intensities of the peaks are lower. Concurrently, the intensity of the palmitic acid ion is higher for specimen B (Figure 4b). Both of these observations suggest that SAM-coated particles from specimen B have more complete coverage. As a reference, the oxidized uncoated particles (specimen C) were also analyzed (Figure 4c). It shows an increase in intensity of the aluminum oxide clusters when compared to the coated particles. The increase can be attributed to the greater thickness of oxide layer on uncoated particles. A comparison of the yields (number of ions emitted per projectile impact) of the most intense cluster in the mass spectrum (described by the formula $[(Al_2O_3)_nAlO_2]^-$) for the different particles further supports the inequality in coverage (Figure 5). The degree of coating cannot be determined as an absolute value, since the signal of secondary ions is a function of ionization/detection efficiency. This efficiency depends on a few variable experimental parameters.[11] However, the relative

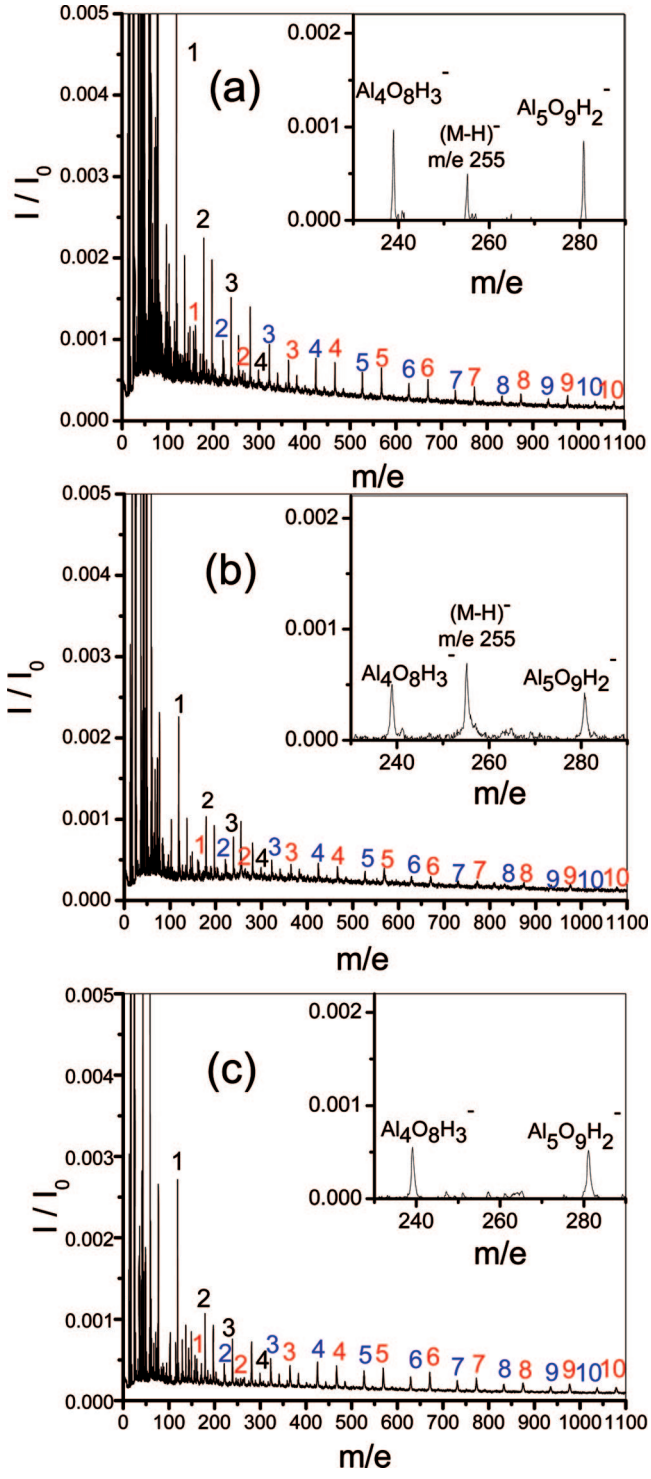

Figure 4. Negative ion mass spectra of (a) specimen A, (b) specimen B, and (c) specimen C obtained under Au_{400}^{4+} bombardment at 136 keV total impact energy. The secondary ions can be classified into different clusters that are color coordinated as follows. The red peaks are clusters with the generic formula $[(Al_2O_3)_nAlO_2]^-$, the blue peaks are clusters identified as $[(Al_2O_3)_nOH]^-$, and the black peaks are clusters with formula $[AlO_2(AlO)_n(OH)_n]^-$, where n in each case is an integer. The peak intensities (I) are normalized to the total number of projectiles I_0 on the y-axis. The insets represent a magnified version of the mass range from 230 to 290, after background subtraction. The deprotonated molecule of the palmitic acid is present in specimens A and B between the clusters represented by the formula $[AlO_2(AlO)_3(OH)_3]^-$ (in figure $Al_4O_8H_3$) and $[(Al_2O_3)_2(AlO)(OH)_2]^-$ (in figure $Al_5O_9H_2$) but absent in specimen C.

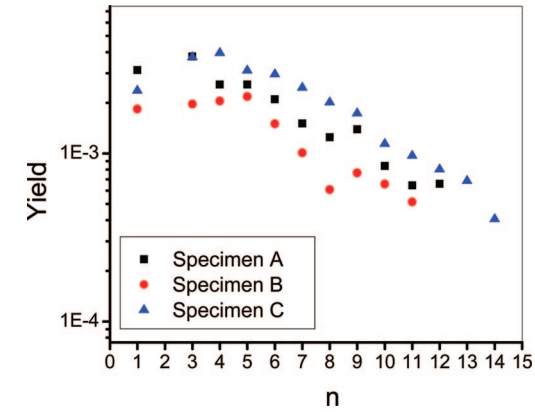

Figure 5. Trends in the yields for the 50 nm coated particles (specimen A), the 100 nm coated particles (specimen B), and the 50 nm oxidized particles (specimen C) as a function of integer n in the cluster group $[(Al_2O_3)_nAlO_2]^-$ with Au_{400}^{4+} at 136 keV total impact energy.

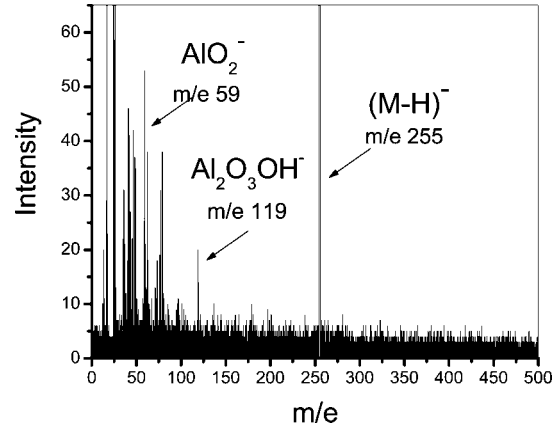

Figure 6. Negative ion mass spectrum of ions coemitted with palmitic acid ion (specimen A). The mass spectrum was acquired with ~2 million impacts of 136 keV Au_{400}^{4+}.

degree of coating, β, can be extracted from the experimental data

$$\beta = \left(\frac{N_{M-H}}{n_0}\right)_A \Big/ \left(\frac{N_{M-H}}{n_0}\right)_B = \frac{p_A}{p_B} \quad (1)$$

where N_{M-H} denotes the number of deprotonated palmitic acid ions $(M-H)^-$ detected (net peak area) and n_0 is the total number of projectile impacts. The degree of coating, p, is $p = S_{M-H}/S_0 = n_{M-H}/n_0$, where S_0 is the average surface area of a nanoparticle, S_{M-H} is the average coated area, and n_{M-H} is the number of projectile impacts on the coated areas. The comparison of the specimens A and B gives $\beta = 0.7 \pm 0.05$. Thus, the particles from specimen B have a better SAM coverage. The average uncoated area of the particles from specimen A is at least 30%.

As noted at the outset, the ability to detect individual mass spectra corresponding to the SAM area of the nanoparticles prompts questions about the relative thickness of the different oxide layers (the layer beneath the SAM and the layer from an uncoated area) and about the effect of exposure to air on the thicknesses of these layers. It must be noted that variations in oxide thickness may be detected within the depth of SI emission. Thus, oxidation beyond ~10 nm will not be recognized.

Table 1. Yields of Aluminum Oxide Cluster Ions Emitted from Specimens A and B[a]

	Y_{A1O_2}	Y'_{A1O_2}	$(Y_{A1O_2})_A / (Y_{A1O_2})_B$	$(Y'_{A1O_2})_A / (Y'_{A1O_2B}$
A	0.11 ± 0.01	0.13 ± 0.01	1.9 ± 0.2	2.0 ± 0.2
B	0.06 ± 0.005	0.07 ± 0.005		

[a] The yield, Y_{A1O_2}, corresponds to the total surface of the nanoparticle (SAM coated and uncoated). Y'_{A1O_2} is the yield of ions emitted from the SAM coated area. The accuracy of yield measurements is ±10%.

The value of the relative thickness of the oxide layer beneath the SAM can be extracted from the experimental data by the following calculations. The number of deprotonated palmitic acid ions $(M-H)^-$ detected, N_{M-H}, can be expressed as

$$N_{M-H} = n_{M-H} Y_{M-H} \tag{2}$$

where Y_{M-H} is the yield of $(M-H)^-$. Similarly, N'_{A1O_2} is the detected number of aluminum oxide ions $(AlO_2)^-$ which were emitted from coated areas

$$N'_{AlO_2} = n_{M-H} Y'_{AlO_2} \tag{3}$$

where Y'_{A1O_2} is the yield of $(AlO_2)^-$ emitted from coated areas. The coemission of $(M-H)^-$ with aluminum oxide ion $(AlO_2)^-$ represented by $N_{A1O_2,M-H}$ can be expressed as

$$N_{AlO_2,M-H} = n_{M-H} Y_{AlO_2,M-H} \tag{4}$$

Considering that for cluster bombardment $Y_{A1O_2,M-H} = Y'_{A1O_2} Y_{M-H}$,[12] the combination of expressions 2, 3, and 4 gives

$$Y'_{AlO_2} = N_{AlO_2,\ M-H} / N_{M-H} \tag{5}$$

As indicated earlier, the emission depth of secondary ions is ≤10 nm. The thickness of the self-assembled monolayer is well-defined (length of palmitic acid chain is of ~3 nm). Thus, the yield Y'_{A1O_2} reflects the thickness of the aluminum oxide interface layer beneath the SAM. One further important comment is that Y'_{A1O_2} is independent of the number of projectiles hitting the SAM area of nanoparticles. Values of Y'_{A1O_2} from different samples can thus be directly compared. Expressions 3−5 are suitable for any sort of aluminum oxide cluster ions coemitted with palmitic acid ions, e.g., $(Al_2O_3)OH^-$ (Figure 6).

The yield of aluminum oxide ions emitted from the total surface (area beneath the SAM and uncoated area) of the nanoparticles can again be calculated from the data of the number of the coemitted aluminum oxide cluster ions of the different type, e.g., AlO_2^- and $(Al_2O_3)OH^-$:

$$Y_{AlO_2} = N_{AlO_2,Al_2O_3OH} / N_{Al_2O_3OH} \tag{6}$$

The yields Y'_{A1O_2} and Y_{A1O_2} calculated for specimens A and B are shown in Table 1. The ratio of yields, Y'_{A1O_2}/Y_{A1O_2}, which is ~1 for both specimens, indicates that short exposure in the air (~10 min) does not increase the degree of oxidation of the uncoated areas. The ratios of yields $(Y_{A1O_2})_A/(Y_{A1O_2})_B$ and $(Y'_{A1O_2})_A/(Y'_{A1O_2})_B$, which are ~2, show that the better coated nanoparticles from specimen B ($\beta = 0.7$) have half the thickness of the oxide layer.

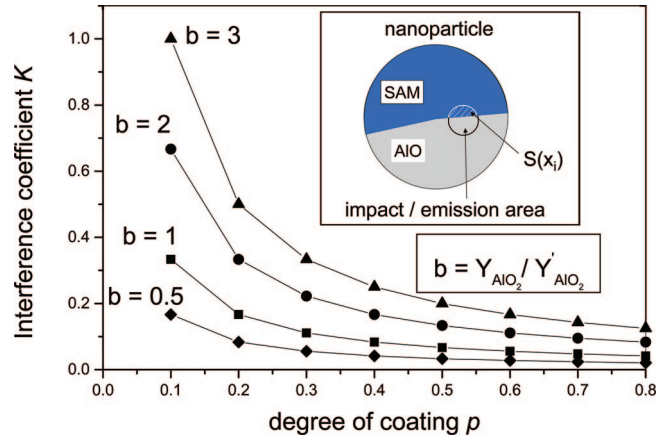

Figure 7. "Interference coefficient" K as a function of the degree of particle coating p.

Obviously, the single impact technique is only meaningful if the nanovolume sampled with a single projectile impact is smaller than the size of the nanoparticle. Nevertheless, one must assess the contribution of interfacial impacts, i.e., projectile impacts on the boundaries between surface areas of SAM and uncoated aluminum oxides. The magnitude of the interfacial contribution can be evaluated with an "interference coefficient" which can be defined as

$$K = \frac{(N_{AlO_2,M-H})_{int}}{N_{AlO_2,M-H}} \tag{7}$$

where $(N_{A1O_2},M-H)_{int}$ is the interfacial contribution, i.e., the number of aluminum oxide ions emitted from the uncoated areas and detected as coemitted with palmitic acid ion; $N_{A1O_2},M-H$ is the number of aluminum oxide ions emitted from SAM areas and detected as coemitted with palmitic acid ion. To calculate K, we use a model of interference where the interference area at the surface of nanoparticle, S_{int}, is larger than the interference area between neighboring nanoparticles (apposition of spherical objects). Considering that $n_{int}/n_{M-H} = S_{int}/S_{SAM}$, where n_{int} is the number of impacts on the interference area and S_{SAM} is the area of nanoparticle coated by SAM, we obtain

$$K = \frac{Y_{AlO_2}}{Y'_{AlO_2} n_{M-H}} \sum_{i=1}^{n_{int}} \frac{x_i d - x_i^2}{d^2} \tag{8}$$

where d is the diameter of the emission area (~10 nm), and x_i is the random distance between the point of impact and the boundary of SAM ($d \geq x_i \geq 0$).

The values of K vs the degree of coating, p, are given in Figure 7. Using Figure 7 one can estimate the accuracy of the single impact measurements. K should be smaller than the precision of our experiment (±10%). For the large variations of the ratio Y_{A1O_2}/Y'_{A1O_2}, K is below 0.2 when the degree of coating is not too low ($p \geq 0.4$). Thus, the spatial resolution of the technique is approximately twice that of the diameter of the emission area (~10 nm). The accuracy of the single impact measurements becomes

unacceptable for oxidized nanoparticles having largely deficient SAM coverage ($K > 0.2$, $p < 0.4$).

SIMS in the mode of single cluster impacts uniquely combines the analytical versatility of surface mass spectrometry with ~20 nm spatial resolution. The method requires a large number of impacts ($\sim 10^6$) to obtain analytically significant information. Yet its "nanoprobe" feature is retained by analyzing the ionized ejecta from each impact independently. The detection limit, under the experimental conditions of this study, is $\sim 10^2$ amol for small molecular weight organics such as palmitic acid. The scope of applications remains to be explored. The method should be useful for determining if further oxidation occurs in SAM-protected areas under prolonged air exposure. For instance, do the uncoated areas stimulate oxidation beneath those covered by SAM? It can also examine the relationship between the initial oxide thickness and the quality of the SAM coverage. An important added capability, namely, the combination of the single projectile impacts with the concurrent real-time localization of each impact, is in progress.

Acknowledgment. This work was supported by the National Science Foundation (Grant CHE-0449312) and the Robert A. Welch Foundation (Grant A-1482). We thank Dr. L. Kaledin from Argonide Corporation for helpful discussions and supplying the samples. The field emission SEM acquisition was supported by the National Science Foundation under Grant No.DBI-0116835.

References

(1) Verkhoturov, S. V.; Rickman, R. D.; Guillermier, C.; Hager, G. J.; Locklear, J. E.; Schweikert, E. A. *Appl. Surf. Sci.* **2006**, *252*, 6490.
(2) Tempez, A.; Schultz, J. A.; Della-Negra, S.; Depauw, J.; Jacquet, D.; Novikov, A.; Lebeyec, Y.; Pautrat, M.; Caroff, M.; Ugarov, M.; Bensaoula, H.; Gonin, M.; Fuhrer, K.; Woods, A. *Rapid Commun. Mass Spectrom.* **2004**, *18*, 371.
(3) Li, Zhen; Verkhoturov, S. V.; Schweikert, E. A *Anal. Chem.* **2006**, *78*, 7410.
(4) Delcorte, A.; Garrison, B. J. *J. Phys. Chem. C* **2007**, *111*, 15312.
(5) Verkhoturov, S. V.; Rickman, R. D.; Balderas, S.; Schweikert, E. A. *Appl. Surf. Sci.* **2004**, *231–232*, 113.
(6) Park, M. A.; Gibson, K. A.; Quinones, L.; Schweikert, E. A. *Science* **1990**, *248*, 988.
(7) Rickman, R. D.; Verkhoturov, S. V.; Hager, G. J.; Schweikert, E. A. *Int. J. Mass Spectrom. Ion Phys.* **2005**, *245*, 48.
(8) Bouneau, S.; Della-Negra, S.; Depauw, J.; Jacquet, D.; Le Beyec, Y.; Mouffron, J. P.; Novikov, A.; Pautrat, M *Nucl. Instrum. Methods Phys. Res., Sect. B* **2004**, *225*, 579.
(9) Rickman, R. D.; Verkhoturov, S. V.; Hager, G. J.; Schweikert, E. A.; Bennet, J. A. *Int. J. Mass Spectrom. Ion Phys.* **2005**, *241*, 57.
(10) Verdier, S.; Metson, J. B.; Dunlop, H. M. *J. Mass Spectrom.* **2007**, *42*, 11.
(11) Witmaack, K. Quantitative analysis of solids by SIMS and SNMS. In *Quantitative Microbeam Analysis*; Fitzgerald, A. G.; Storey, B. E.; Fabian, D., Eds.; IOP Publishing Ltd: London, 1993; Chapter 1.
(12) Rickman, R. D.; Verkhoturov, S. V.; Parilis, E. S.; Schweikert, E. A. *Phys. Rev. Lett.* **2004**, *92*, 04760.

NL0730716